Throughput Calculation in a HIPERLAN Type 2 Network Considering Power Control and Link Adaptation

Markus Radimirsch, Klaus Jobmann

Abstract

This paper deals with the combination of transmit power control and link adaptation in wireless data networks. The tools for engineering wireless voice networks are not necessarily suited for data communications due to the smooth transition between good and bad state in data networks. This paper proposes a theoretical model to calculate the throughput in a wireless data network, using HIPERLAN type 2 as example system. It is based on the computation of the probability density function of the signal-to-interference ratio (SIR) at the receiver and calculation of the expected throughput value, based on known throughput curves versus SIR. The results from the theoretical model are presented and compared to results from a simulation model. An important outcome is that the maximum throughput in the network is not necessarily achieved at maximum transmit powers.

Index terms

Wireless data networks, Link adaptation, power control, system investigation, HIPERLAN type 2, throughput model, theory, simulation

I. Introduction

An important quality parameter in engineering wireless voice networks, such as the GSM network, is the percentage of the coverage area where the achievable signal-to-interference ratio (SIR) is above a minimum value. This minimum value is usually defined by a maximum allowed bit or packet error rate which still guarantees a minimum level of the communication quality perceived. This can be translated into a utility function, i.e. a function which indicates the usefulness of an SIR level to the user. An example utility function for voice services is shown in

fig. 1, as e.g. proposed in [1]. The statement of this utility function is that the full utility is given above the SIR threshold, whereas the utility drops abruptly to zero below the threshold SIR. Note that this may not be an exact model but it is the one used to dimension voice networks.

The inverse of the covered area with sufficient SIR are areas where users cannot get a service with sufficient quality, so-called outage areas. For radio voice networks with regular structure, the Interference Reduction Factor (IRF), [2, sec. 2.3.2], which uses the utility function for voice in fig. 1, can be used to determine the required frequency reuse distance between radio cells with a certain radius, a given required SIR and an outage probability. It is a popular initial estimate in voice radio network planning. The IRF, however, is not well suited for many wireless *data* networks. This is especially true if the perceived quality degrades smoothly with decreasing SIR. A possible quality measure is the user throughput. With an automatic repeat request (ARQ) scheme, the throughput $\mathcal{T}$ is given as a function of the packet error rate (PER), which is a function of the SIR, and the raw data rate on the physical layer, $\mathcal{R}$.

An example utility function for data networking, based on the throughput, has been proposed in [1] and is shown in fig. 1. It expresses the fact that e.g. a web user is entirely satisfied, as long as the web pages appear ”quick enough”. He gets more and more unsatisfied, as the delay becomes longer, until he finally stops using the web because the waiting time becomes unacceptable. This satisfaction is closely connected with the achievable throughput and the resulting delay.

So the methods to engineer wireless voice networks are not necessarily suited for wireless data networks. This paper proposes a new evaluation method, using the throughput as utility. It relies on HIPERLAN/2 as the underlying technology, [3]. However, the basic approach is widely generic and can be re-used for other network technologies.

The main achievement of this paper is a theoretical model to evaluate network throughput. TPC parameters are fixed for each experiment, where the influence of power control is considered by performing many experiments with different TPC parameter combinations, i.e. it is only LA which is dynamic in this paper. As is well known, radio network investigations have to

take into account a huge number of parameters, making it difficult, if not impossible, to find analytical models. The analytical model proposed in this paper, therefore, has been developed for a simplified regular scenario with circular radio cells, equal spatial distribution of terminals inside cells and with a deterministic propagation model.

The chosen scenario reflects most properties of radio networks. This means that the model can be used to derive an indication of radio network behaviour but is not suited for dimensioning of network installations. A comparable measure in the domain of voice networks is the IRF which is based on similar assumptions as the model in this paper. The IRF is commonly used for an inital indication of basic network parameters but is too simplistic for final network planning. The advantage of such analytical models is that, compared with e.g. simulation models, they are simple and require only little time to yield initial results.

For convenience, we will introduce some technical features of the HIPERLAN/2 system in section 2, especially with respect to its link adaptation (LA) and Transmit Power Control (TPC) mechanisms. Some related work will also be mentioned in this section. Analytical models for the throughput calculation in different interference scenarios will be developed in section 3. The results from these models will be compared with a computer simulation model in section 4.

II. Some basics and related work

A. Basics of HIPERLAN Type 2

A number of publications about HIPERLAN Type 2 (H2) is available, such as [3], [4]. The explanations given here are only what is necessary for the understanding of this paper.

LA is the ability to transmit high data rates when the channel is good, i.e. at high SIR, and low data rates at bad channel conditions, i.e. at low SIR. It is mainly the physical layer of H2 that supports LA. Seven Phy modes exist, as defined in [5][1].

[1]The Phy mode with 9 Mbit/s is not used here because it has worse performance than the one with 12 Mbit/s

Each Phy mode PM has its raw data rate $\mathcal{R}_{PM}$. However, with decreasing SIR, the share of packets that are received with errors, increases. H2 provides a selective repeat ARQ which retransmits incorrect packets. With the PER and $\mathcal{R}_{PM}$, the useful throughput after ARQ, $\mathcal{T}_{PM}$, is given by:

$$\mathcal{T}_{PM} = \mathcal{R}_{PM} \cdot (1 - \mathrm{PER}) \,. \tag{1}$$

The throughput curves that are used throughout this paper are taken from [3] and are shown in fig. 2. They are approximated with the functions in [6] for all investigations in this paper. Note that the envelope of the curves is similar to the utility function for wireless data networks in fig. 1. Obviously, the highest possible throughput in a system with interference can be achieved by always selecting the Phy mode with the highest throughput for the current γ, denoted as $\mathcal{T}_{\max_\gamma(PM)}$, where γ is another notation for SIR. We define $\mathcal{R}_{\max_\gamma(PM)}$, the function which always selects the Phy mode with the highest throughput for a given γ.

H2 is a connection oriented system with a central medium access control (MAC), where an access point (AP) determines and announces its transmissions in the downlink (DL) and those of mobile terminals (MT) in the uplink (UL). The air interface is divided in MAC frames of equal duration and the scheduled transmissions can vary from MAC frame to MAC frame. The AP scheduler has knowledge about the amount of data in each buffer that waits to be transmitted and allocates transmission opportunities to connections. During scheduling, the AP has to take into account the Phy mode each connection has in UL and DL. Since scheduling is not in the focus of this paper, we will not go into detail on this subject. For further discussion see e.g. [7]. The scheduling scheme used in this publication tries to find a balance between allocation of time shares and amount of data. We assume N_c active connections and each connection $i, i \in 1...N_c$ uses the Phy mode PM_i with raw data rate $\mathcal{R}_{PM_i}$. The scheduling strategy works such that the time share of connection i is proportional to F_{PM_i}, where

$$F_{PM_i} = \sqrt{\frac{54\text{Mbit/s}}{\mathcal{R}_{PM_i}}} \tag{2}$$

As we will see later, F_{PM_i} contains all we need in the mathematical models to represent the scheduling scheme, so the models are applicable to any scheduler for which F_{PM_i} can be computed. The only justification for the specific choice in this paper is that some scheduling scheme had to be chosen, among others with the purpose to make simulation and theoretical models comparable. It is worth mentioning that the results in subsequent sections have been obtained for this specific choice of a scheduling scheme and that other scheduling schemes may lead to different outcomes.

For the purpose of TPC, the AP transmits with constant transmit power $P_{t,\mathrm{AP}}$ during a MAC frame, where $P_{t,\mathrm{AP}}$ can vary from MAC frame to MAC frame. Moreover, the AP broadcasts $P_{t,\mathrm{AP}}$ in each MAC frame, together with its expected receive power $P_{e,\mathrm{AP}}$. The mobile terminal (MT) can calculate the path loss L from the received power level $P_{r,\mathrm{MT}}$ and from $P_{t,\mathrm{AP}}$ to adjust its transmit power $P_{t,\mathrm{MT}}$ to the required level.

B. Related work

This paper deals with the combination of LA and TPC. Some empirical models for this combination have been published earlier, see e.g. [8].

Another method exploits the fact that a MAC frame has a certain capacity. If the available capacity is more than what is required, i.e. all packets in all buffers can be served, some part of the MAC frame stays empty. Together with the facts that the SIR increases with increasing transmit power and that the throughput increases monotonically with the SIR, see fig. 2, the capacity of a MAC frame can be decreased by decreasing and increased by increasing transmit powers. So if the previous MAC frames have significant empty parts, $P_{t,\mathrm{AP}}$ and $P_{e,\mathrm{AP}}$ can be decreased. Such schemes have been published in [9], [10]. The scheme in [9] uses a mechanism in H2 which was originally designed to equalise inaccuracies in the RF part, to adapt the transmit power of individual MTs. The investigations are for a partly loaded network. In [10], the original H2 TPC scheme has been used, and the investigations are for a network under high load conditions.

The point with these schemes is that they both decrease transmit powers only if the load in

the network is lower than the maximum capacity. If the full capacity is required, $P_{t,\mathrm{AP}}$ and $P_{e,\mathrm{AP}}$ are set to the maximum value. However, it is not clear whether, under mutual interference, using maximum powers leads to maximum network throughput.

This paper deals with a model to evaluate the network throughput under overload conditions. One major goal is to answer the question left open by [9], [10], i.e. to find out at which combination of $P_{t,\mathrm{AP}}$ and $P_{e,\mathrm{AP}}$ we get the maximum network throughput. For this purpose, TPC is switched off, i.e. we have fixed values for $P_{t,\mathrm{AP}}$ and $P_{e,\mathrm{AP}}$ in our models. However, LA is still used in the sense of $\mathcal{R}_{\max_\gamma(PM)}$.

III. Throughput Models

This section presents three throughput models. The first model considers the case where only a single radio cell is present, i.e. there are no interfering cells in its surrounding. For this case, we can give a fully mathematical model. The second case deals with two radio cells where one of them is the observed cell and the second one is the interfering cell. We will develop a semi-analytical model for this case which is evaluated numerically. The third model is for the case of a regular radio network which considers more than one interfering cell. This model is an approximation, based on the semi-analytical model for the case of one interfering cell. These models represent cases, where the dynamic frequency selection of H2 works fine, down to situations with high network density, possibly with networks from different operators in a limited geographic area.

The models use a two-slope path loss model which does not consider slow or fast fading, [11]. Let ρ be the distance between transmitter and receiver and the pathloss L a function of ρ, $L(\rho)$. Then

$$L/\mathrm{dB} = \begin{cases} a_1 + b_1 \cdot \log_{10} \rho/\mathrm{m}; & 0 \le \rho \le 5\,\mathrm{m} \\ a_2 + b_2 \cdot \log_{10} \rho/\mathrm{m}; & \rho > 5\,\mathrm{m} \end{cases} \tag{3}$$

where $a_1 = 46$, $b_1 = 20$, $a_2 = 36$ and $b_2 = 35$. The model assumes line-of-sight propagation in the proximity of the transmitter at distances below $5\,\mathrm{m}$, whereas obstacles exist for higher

distances, leading to a power-of 3.5 law. This model fits well office or home environments with small to medium sized rooms. We further assume that the AP is mounted on the ceiling which leads to a minimal distance $\rho_{\min} = 2\,\mathrm{m}$ between transmitter and receiver.

We assume background noise N_0 for all investigations. Its level results from a simple link budget analysis, [12, sec. 5.5.2]. Starting with a basic background noise of -174 dBm, taking into account the H2 channel bandwidth B of 20 MHz and receiver noise N_E =6 dB, we get[2]:

$$\frac{N_0}{\mathrm{dBm}} = -174 + 10\log_{10}(\frac{B}{\mathrm{Hz}}) + \frac{N_E}{\mathrm{dB}} = -95 \tag{4}$$

The principle behind all three throughput models is to compute the probability density function (pdf) of γ, $f_\gamma(\gamma)$, at the receiver and to use the throughput curves from fig. 2 to calculate the expected value of the throughput in UL and DL, provided that we always use $\mathcal{R}_{\max_\gamma(PM)}$. A prerequisite is that there are always packets to transmit, i.e. the model assumes a high load case. However, the influence of the scheduler, as defined in (2), has to be taken into account, since it determines the transmission time share of a terminal with a certain γ.

Definition: We define the time norm of $f_\gamma(\gamma)$ as:

$$\tau_{\mathrm{norm}} = \int_0^\infty f_\gamma(\gamma) \cdot F_{\max_\gamma(PM)}(\gamma)\,\mathrm{d}\gamma \tag{5}$$

Note that $F_{\max_\gamma(PM)}(\gamma)/\tau_{\mathrm{norm}} = \mathrm{Prob}(PM|\gamma)$, i.e. the probability that a Phy mode is used, conditioned on γ. The wheighted pdf of γ, taking into account the effect of the used scheduling strategy, is defined as:

$$f_{PM}(\gamma) = \frac{1}{\tau_{\mathrm{norm}}} f_\gamma(\gamma) \cdot F_{\max_\gamma(PM)}(\gamma) \tag{6}$$

Theorem 1 *: With $\mathcal{T}_{PM}(\gamma)$ according to (1), the expected value for the maximally achievable throughput $\mathcal{T}_{\max}$ of the observed radio cell with $f_{PM}(\gamma)$ is:*

$$E\{\mathcal{T}_{\max}\} = \int_0^\infty f_{PM}(\gamma) \cdot \mathcal{T}_{max_\gamma(PM)}(\gamma) \cdot\ \mathrm{d}\gamma \tag{7}$$

[2]If not stated otherwise, all absolute power levels are given in dBm and all relative power levels, such as the path loss L, in dB in the remainder of the paper.

Proof: (7) describes the computation of an expected value with $\gamma \in \mathbb{R}^+$.

$\triangle$

Theorem 1 is the basis for all subsequent models. So what remains to be done is to determine $f_\gamma(\gamma)$. The following sections will develop models for the computation of $f_\gamma(\gamma)$ for the three cases listed at the beginning of this section. Note that the scheduling scheme is considered only by $\mathrm{Prob}(PM|\gamma)$. So the model is able to cope with any scheduling scheme, as long as $\mathrm{Prob}(PM|\gamma)$ can be computed.

A. Throughput calculation for a single radio cell

If we have only one radio cell operating on one frequency, the limiting factor is the background noise N_0. We assume that the MT has a maximum transmit power limit $P_{t,\mathrm{MT},max}$ which it cannot exceed. If not stated otherwise, $P_{t,\mathrm{MT},max}$ will be set to 23 dBm in the sequel. With pathloss L, then, $P_{t,\mathrm{MT}}$ is calculated as:

$$P_{t,\mathrm{MT}} = \begin{cases} P_{e,\mathrm{AP}} + L\,; & P_{e,\mathrm{AP}} + L \le P_{t,\mathrm{MT},max} \\ P_{t,\mathrm{MT},max}\,; & \text{otherwise} \end{cases} \tag{8}$$

If we use the pathloss model in (3), we can express $P_{t,\mathrm{MT}}$ as a function of the distance ρ:

$$P_{t,\mathrm{MT}} = \begin{cases} P_{e,\mathrm{AP}} + a_1 + b_1 \cdot \log_{10}(\rho/\mathrm{m}); & \rho_{\min} \le \rho \le 5\mathrm{m} \\ P_{e,\mathrm{AP}} + a_2 + b_2 \cdot \log_{10}(\rho/\mathrm{m}); & 5\mathrm{m} < \rho \le 10^{\left(P_{t,\mathrm{MT},max} - a_2 - P_{e,\mathrm{AP}}\right)/b_2}\ \mathrm{m} \\ P_{t,\mathrm{MT},max}\,; & \text{otherwise} \end{cases} \tag{9}$$

$P_{t,\mathrm{AP}}$ can be adjusted in 3 dB steps from -15 dBm to 30 dBm, $P_{e,\mathrm{AP}}$ in 4 dB steps from -71 dBm to -43 dBm, [5]. Considering (8), we get for the AP reception power $P_{r,\mathrm{AP}}$:

$$P_{r,\mathrm{AP}} = \begin{cases} P_{e,\mathrm{AP}}; & \rho_{\min} \le \rho \le 10^{\left(P_{t,\mathrm{MT},max} - a_2 - P_{e,\mathrm{AP}}\right)/b_2}\ \mathrm{m} \\ P_{t,\mathrm{MT},max} - a_2 - b_2 \cdot \log_{10}(\rho/\mathrm{m}); & \rho \ge 10^{\left(P_{t,\mathrm{MT},max} - a_2 - P_{e,\mathrm{AP}}\right)/b_2}\ \mathrm{m} \end{cases} \tag{10}$$

Definition: We assume that the MTs move equally distributed within a circle of radius R around the AP and that $\delta(\cdot)$ is the Dirac impuls. Let

$$f^{(1)}_{\gamma_{\mathrm{AP},0}}(\gamma) = \min\left\{1,\ \frac{1}{R^2 - \rho^2_{\min}} \cdot \left[10^{2\cdot(P_{t,\mathrm{MT},max} - a_2 - P_{e,\mathrm{AP}})/b_2} - 4\right]\right\} \cdot \delta(P_{e,\mathrm{AP}} - N_0) \tag{11}$$

and:

$$f^{(2)}_{\gamma_{\mathrm{AP},0}}(\gamma) = \begin{cases} \frac{2\ln 10}{b_2(R^2-\rho^2_{\min})} \cdot \left[10^{2\cdot(P_{t,\mathrm{MT},max}-a_2-\gamma-N_0)/b_2} - 4\right]; & \\ & P_{r,\mathrm{AP}}(R) - N_0 \le \gamma < P_{e,\mathrm{AP}} - N_0 \\ 0\,; & \text{otherwise} \end{cases} \tag{12}$$

Lemma 1 *: The pdf for the SIR at the AP without interference of surrounding radio cells is given by:*

$$f_{\gamma_{\mathrm{AP},0}}(\gamma) = f^{(1)}_{\gamma_{\mathrm{AP},0}}(\gamma) + f^{(2)}_{\gamma_{\mathrm{AP},0}}(\gamma). \tag{13}$$

Proof: The detailed proof is given in appendix I. The expression in (11) is repsonsible for the constant part in (10), whereas (12) is responsible for the decreasing part in (10).

The situation in the DL is analogous. The transmit power of the AP is constant during a MAC frame. With the pathloss in (3), we get the receive power at the MT:

$$P_{r,\mathrm{MT}}(\rho) = P_{t,\mathrm{AP}} - L(\rho) = \begin{cases} P_{t,\mathrm{AP}} - a_1 - b_1 \cdot \log_{10}\rho/\mathrm{m}; & 0 \le \rho \le 5\mathrm{m} \\ P_{t,\mathrm{AP}} - a_2 - b_2 \cdot \log_{10}\rho/\mathrm{m}; & \rho > 5\mathrm{m} \end{cases} \tag{14}$$

Lemma 2 *: The pdf of the SIR in the DL in a single radio cell is:*

$$f_{\gamma_{\mathrm{MT},0}}(\gamma) = \begin{cases} \frac{2\ln 10}{b_1(R^2-\rho^2_{\min})} \cdot 10^{2\cdot(P_{t,\mathrm{AP}}-a_1-\gamma)/b_1}; & \\ & P_{r,\mathrm{MT}}(\rho_{\min}) - N_0 \ge \gamma > P_{r,\mathrm{MT}}(5\,\mathrm{m}) - N_0 \\ \frac{2\ln 10}{b_2(R^2-\rho^2_{\min}))} \cdot 10^{2\cdot(P_{t,\mathrm{AP}}-a_2-\gamma)/b_2}; & \\ & \gamma \le P_{r,\mathrm{MT}}(5\,\mathrm{m}) - N_0 \end{cases} \tag{15}$$

Proof: The proof is similar to the proof of $f^{(1)}_{\gamma_{\mathrm{AP},0}}(\gamma)$ in Lemma 1, see appendix I.

△

With the pdfs $f_\gamma(\gamma)$ for AP and MT, we have everything to calculate the possible throughput in UL and DL with the help of (7). The total throughput in the UL, $\mathcal{T}_{\mathrm{tot,UL}}$, is listed in table I and in the DL, $\mathcal{T}_{\mathrm{tot,DL}}$, in table II. The throughput entries in tables I and II are derived under the assumption that a terminal that moves equally distributed in the radio cell, transmits or receives permanently without overhead and interruption, meaning that there is no traffic in the opposite direction. Note that this is not achievable in reality.

The variation of $P_{e,\mathrm{AP}}$ down to $-63\mathrm{dBm}$ has no significant effect on the throughput, the effect below $-63\,\mathrm{dBm}$ is quite small. On the other hand, the variation of $P_{t,\mathrm{AP}}$ affects throughput in the DL significantly. As can be expected, the throughput generally decreases with increasing R.

B. Model for two radio cells

We extend the model introduced in section III-A such that it is applied to the situation where, in addition to the observed cell, a second radio cell is present that generates interference on the same frequency. Both cells have circular areas with radii R_1 and R_2, where we have $R_1 = R_2 = R$. The APs are located in the centers of the cells. MTs move equally distributed inside the circles around the AP. The cartesian coordinates of the APs are $(0, 0)$ for AP_1 in the observed cell and $(D, 0)$ for AP_2, i.e. their distance is D. The coordinates of the MTs are given in polar coordinates with the distance to the respective AP, ρ_1 and ρ_2, and their angles, ϕ_1 and ϕ_2, where $\rho_1, \rho_2 \in [\rho_{\min}, R]$ and $\phi_1, \phi_2 \in [0, 2\pi[$. This means that an MT in cell 1 has the cartesian coordinates $(x_1, y_1) = (\rho_1 \cos\phi 1, \rho_1 \sin\phi 1)$ and in cell 2 $(x_2, y_2) = (D + \rho_2 \cos\phi 2, \rho_2 \sin\phi 2)$.

With P_i^{lin} the interference power, P_r^{lin} the reception power at the receiver, N_0^{lin} the noise power and L^{lin} the pathloss, all in linear representation, we get for γ in dB:

$$\gamma = 10 \cdot \log_{10}\left(\frac{P_r^{\text{lin}}}{P_i^{\text{lin}} + N_0^{\text{lin}}}\right) \tag{16}$$

Again, our goal is to derive the pdf of γ in UL and DL in the observed cell, given the interference in the second cell. Once we have the pdf of γ, we can determine the throughput with (7). It is very difficult, if not impossible, to calculate the pdf of γ analytically. Therefore, the proposed model is a semi-analytical method. We assume that $P_{t,\mathrm{AP}}$ and $P_{e,\mathrm{AP}}$ are given and assumed to be equal in both radio cells for the explanations below. Further, ρ_1, ϕ_1, ρ_2 and ϕ_2 can take on discrete values with stepwidths $\Delta\rho_1, \Delta\phi_1, \Delta\rho_2$ and $\Delta\phi_2$.

The throughput in the observed cell depends on the interference generated by the AP and the MTs in the interfering cell. We need to distinguish four different scenarios:

1) Interference at MTs in observed cell generated by MTs in interfering cell

2) Interference at MTs in observed cell generated by AP in interfering cell

3) Interference at AP in observed cell generated by MTs in interfering cell

4) Interference at AP in observed cell generated by AP in interfering cell

We first consider case 1, the interference at MTs in cell 1 generated by MTs in cell 2.

Definition: Let $P_{r,\mathrm{MT}_1}(\rho_1)$ be the reception power at an MT in cell 1 (MT_1) with distance ρ_1 to the AP in cell 1 (AP_1) according to (14) and $P_{t,\mathrm{MT}_2}(\rho_2)$ the transmit power of an MT in cell 2 (MT_2) with distance ρ_2 to its AP according to (9). We further denote the euclidian distance between MT_1 and MT_2 as $d_{\mathrm{MT}_1,\mathrm{MT}_2}$. Assuming that $D - 2\,R > 5\,\mathrm{m}$, this leads to the pathloss between MT_1 and MT_2:

$$L_{\mathrm{MT}_1,\mathrm{MT}_2}(\rho_1,\phi_1,\rho_2,\phi_2) = a_2 + b_2 \cdot \log_{10} d_{\mathrm{MT}_1,\mathrm{MT}_2}\,, \tag{17}$$

see (3). For convenience, we will omit the indexes and write MT,MT instead of $\mathrm{MT}_1,\mathrm{MT}_2$.

With the linear versions of all variables denoted with $^{\text{lin}}$, the interference power $P^{\text{lin}}_{i,\mathrm{MT},\mathrm{MT}}$, then, is

$$P^{\text{lin}}_{i,\mathrm{MT},\mathrm{MT}}(\rho_1,\phi_1,\rho_2,\phi_2) = \frac{P^{\text{lin}}_{t,\mathrm{MT}_2}(\rho_2)}{L^{\text{lin}}_{\mathrm{MT},\mathrm{MT}}(\rho_1,\phi_1,\rho_2,\phi_2)} \tag{18}$$

We assume the activity share of MTs in the interfering cell to be α_{MT} and of the AP α_{AP}, i.e. MTs and APs contribute to the interference only with their activity share, leading to the effective interference power $P^{\text{lin}}_{i,\mathrm{MT},\mathrm{MT}} \cdot \alpha_{\mathrm{MT}}$. With (16), we get for the effective SIR $\gamma_{\mathrm{MT},\mathrm{MT}}$ at MT_1, generated by an MT_2:

$$\gamma_{\mathrm{MT},\mathrm{MT}} = 10 \cdot \log_{10}\left(\frac{P^{\text{lin}}_{r,\mathrm{MT}_1}(\rho_1)}{P^{\text{lin}}_{i,\mathrm{MT},\mathrm{MT}}(\rho_1,\phi_1,\rho_2,\phi_2)\cdot\alpha_{\mathrm{MT}} + N_0^{\text{lin}}}\right) \tag{19}$$

We proceed numerically to determine the pdf $f_{\gamma_{\mathrm{MT},\mathrm{MT},1}}(\gamma_{\mathrm{MT},\mathrm{MT}})$, where the 1 in the index stands for $s = 1$ interfering cell. For this purpose, we consider every possible combination $(\rho_1,\phi_1,\rho_2,\phi_2)$ given $(\Delta\rho_1,\Delta\phi_1,\Delta\rho_2,\Delta\phi_2)$. If we make the steps small enough, we obtain an approximation for discrete area elements $\Delta A_1 = \rho_1 \cdot \Delta\rho_1\,\Delta\phi_1$ in cell 1 and $\Delta A_2 = \rho_2 \cdot \Delta\rho_2\,\Delta\phi_2$ in cell 2. The discrete area elements are now related to the areas of the circles, $A_1 = \pi R_1^2$ und

$A_2 = \pi R_2^2$. We get:

$$f_{\gamma_{\mathrm{MT,MT}}}(\gamma_1) = \mathrm{Prob}\{\gamma_1 - \Delta\gamma < \gamma_{\mathrm{MT,MT}}(\rho_1, \phi_1, \rho_2, \phi_2) \leq \gamma_1\} \tag{20}$$

Strictly speaking, we obtain a histograph of $\gamma_{\mathrm{MT,MT}}$, denoted as $\mathrm{hist}_{\gamma_{\mathrm{MT,MT},1}}(\gamma_{\mathrm{MT,MT}})$, where $\gamma_{\mathrm{MT,MT}}$ can have discrete values with distance $\Delta\gamma$.

Lemma 3 *: The histograph* $\mathrm{hist}_{\gamma_{\mathrm{MT,MT}}}(\gamma_1)$ *for* $\{\gamma_1 \mid \gamma_1 = n \cdot \Delta\gamma \quad \forall \quad n \in \mathbb{N}\}$ *is defined as*

$$\mathrm{hist}_{\gamma_{\mathrm{MT,MT},1}}(\gamma_1) = \sum_{\substack{(\rho_1, \phi_1, \rho_2, \phi_2) \\ \gamma_1 - \Delta\gamma < \gamma_{\mathrm{MT,MT}}(\rho_1, \phi_1, \rho_2, \phi_2) \leq \gamma_1}} \frac{\rho_1 \cdot \Delta\rho_1 \, \Delta\phi_1 \;\cdot\; \rho_2 \cdot \Delta\rho_2 \, \Delta\phi_2}{A_1 \cdot A_2} \tag{21}$$

where $\rho_1 \in [\rho_{\min}, R]$, $\rho_2 \in [\rho_{\min}, R]$, $\phi_1 \in [0, 2\pi[$ *and* $\phi_2 \in [0, 2\pi[$.

Proof: Due to the equal distribution in the circular areas, the probability that an MT is located in an area element limited by the points (in polar coordinates) (ρ, ϕ), $(\rho + \Delta\rho, \phi)$, $(\rho, \phi + \Delta\phi)$ and $(\rho + \Delta\rho, \phi + \Delta\phi)$ is the ratio between the discrete area element and the circle areas A_1 and A_2. We get the probabilities $p_{\Delta A_1}(\rho_1, \phi_1)$ and $p_{\Delta A_2}(\rho_2, \phi_2)$:

$$p_{\Delta A_1}(\rho_1, \phi_1) = \frac{\Delta A_1}{A_1} = \frac{\rho_1 \cdot \Delta\rho_1 \, \Delta\phi_1}{2\pi R_1} \tag{22}$$

$$p_{\Delta A_2}(\rho_2, \phi_2) = \frac{\Delta A_2}{A_2} = \frac{\rho_2 \cdot \Delta\rho_2 \, \Delta\phi_2}{2\pi R_2} \tag{23}$$

According to (21), $\mathrm{hist}_{\gamma_{\mathrm{MT,MT},1}}(\gamma_1)$ is the sum over all location combinations in cell 1 and cell 2 for which we have $\gamma_1 - \Delta\gamma < \gamma_{\mathrm{MT,MT}}(\rho_1, \phi_1, \rho_2, \phi_2) \leq \gamma_1$, wheighted with the probability that this location combination occurs, $p_{\Delta A_1}(\rho_1, \phi_1) \cdot p_{\Delta A_1}(\rho_2, \phi_2)$.

$\triangle$

We will assume that the histograph is close enough to the pdf and use the term pdf instead. This is possible, if the stepwidths $\Delta\rho_1$, $\Delta\phi_1$, $\Delta\rho_2$, $\Delta\phi_2$ and $\Delta\gamma$ are sufficiently small[3].

[3]Investigations show that the deviation between results for using half the stepwidth is well below 0.3% for $\Delta\rho \leq 2\,\mathrm{m}$ and for $\Delta\phi \leq 2°$. We have used $\Delta\rho = 1\,\mathrm{m}$ and $\Delta\phi = 0.5°$

The remaining cases for $f_{\gamma_{\mathrm{AP,MT},1}}$ (interference in the observed cell caused by AP in interfering cell) and for interference at the AP in the observed cell, $f_{\gamma_{\mathrm{MT,AP},1}}$ and $f_{\gamma_{\mathrm{AP,AP},1}}$, are determined in a similar way. Note that, despite the constant positions of both APs, $f_{\gamma_{\mathrm{AP,AP},1}}$ is not a single value due to the non-constant receive powers at the AP, cf. (10).

Now we use the time norm in (5) in order to consider the effect of the chosen scheduling strategy. First, we calculate the time norm $\tau_{\mathrm{norm_{MT}}}$ using $f_{\gamma_{\mathrm{MT},1}}(\gamma)$ and $\tau_{\mathrm{norm_{AP}}}$ using $f_{\gamma_{\mathrm{AP},1}}(\gamma)$. The sum of the two time norms results in $\tau_{\mathrm{norm_{tot}}}$. The activity shares of MTs, α_{MT}, and of APs, α_{AP}, in the interfering and the observed cells are calulated as[4]:

$$\begin{aligned} \alpha_{\mathrm{MT}} &= \frac{\tau_{\mathrm{norm_{MT}}}}{\tau_{\mathrm{norm_{tot}}}} \\ \alpha_{\mathrm{AP}} &= \frac{\tau_{\mathrm{norm_{AP}}}}{\tau_{\mathrm{norm_{tot}}}} \end{aligned} \tag{24}$$

The pdf of γ at the MTs in the observed cell is composed by $f_{\gamma_{\mathrm{MT,MT},1}}$ and $f_{\gamma_{\mathrm{AP,MT},1}}$. If we assume the activitiy ratio α_{AP} of the AP and α_{MT} of MTs in the interfering cell, we get:

$$f_{\gamma_{\mathrm{MT},1}}(\gamma) = \alpha_{\mathrm{MT}} \cdot f_{\gamma_{\mathrm{MT,MT},1}}(\gamma) + \alpha_{\mathrm{AP}} \cdot f_{\gamma_{\mathrm{AP,MT},1}}(\gamma) \tag{25}$$

and for $f_{\gamma_{\mathrm{AP},1}}$:

$$f_{\gamma_{\mathrm{AP},1}}(\gamma) = \alpha_{\mathrm{MT}} \cdot f_{\gamma_{\mathrm{MT,AP},1}}(\gamma) + \alpha_{\mathrm{AP}} \cdot f_{\gamma_{\mathrm{AP,AP},1}}(\gamma) \tag{26}$$

Definition: The theoretically possible throughput $\mathcal{T}_{\mathrm{MT},1}$ for reception by the MT in the DL and the AP, $\mathcal{T}_{\mathrm{AP},1}$, in the UL is given by (cf. (7)):

$$\mathcal{T}_{\mathrm{MT},1} = \frac{1}{\tau_{\mathrm{norm_{MT}}}} \cdot \int_0^\infty f_{\gamma_{\mathrm{MT},1}}(\gamma) \cdot \mathcal{T}_{max_\gamma(PM)}(\gamma) \cdot F_{\max_\gamma(PM)}(\gamma)\,\mathrm{d}\,\gamma \tag{27}$$

$$\mathcal{T}_{\mathrm{AP},1} = \frac{1}{\tau_{\mathrm{norm_{AP}}}} \cdot \int_0^\infty f_{\gamma_{\mathrm{AP},1}}(\gamma) \cdot \mathcal{T}_{max_\gamma(PM)}(\gamma) \cdot F_{\max_\gamma(PM)}(\gamma)\,\mathrm{d}\,\gamma \tag{28}$$

Theorem 2 *: The total throughput of a radio cell with the presence of a second interfering cell is:*

$$\mathcal{T}_{\mathrm{tot},1} = \alpha_{\mathrm{AP}} \cdot \mathcal{T}_{\mathrm{MT},1} + \alpha_{\mathrm{MT}} \cdot \mathcal{T}_{\mathrm{AP},1} \tag{29}$$

[4]Note that α_{MT} and α_{AP} have been used earlier in the calculation, see (19), which requires iterative computation. Details are described in [13]

Proof: $\mathcal{T}_{\mathrm{MT},1}$ or $\mathcal{T}_{\mathrm{AP},1}$ is the possible throughput according to (7), if only MTs or the AP is receiving. The probability for MTs to receive is defined by the activity share of the AP, α_{AP}, for the AP to receive by α_{MT}. The summation of the possible throughputs of MTs and AP wheighted with the reception probability is equivalent to the calculation of the expected value, [14].

$\triangle$

C. Model for a network of cells

Now we consider a network consisting of more than two radio cells. We assume that s cells surround the observed cell with equal angular distances and all with distance D to the AP of the observed cell. We will use $s = 4$ in our investigations which is justified by the fact that wireless LANs are often applied in office environments, i.e. in buildings which are long stretched.

We re-use the model developed for $s = 1$, i.e. the model for $s > 1$ is an approximation based on the model for $s = 1$. We start with the DL case where we first observe the spatial SIR distribution for $s = 1$. An example is shown in fig. 3 with contour lines on the bottom of the graph. Similar observations can be made for the minimum SIR caused by MTs in the observed cell. So the SIR in the direction of the interfering cell is lower than on the other side. If we assume a second cell on the left side, the spatial distribution would also drop to the left. This leads to the idea to calculate the SIR in the same way as for $s = 1$ and to use only the SIR samples in the so-called dominated sector which is directed towards the interfering cell.

Secondly, the interference power from all interfering cells adds up at the MTs in the observed cell. With the activity α_{MT} of MTs and α_{AP} of APs in interfering cells, the interference power in the dominated sector is multiplied by $s \cdot \alpha_{\mathrm{MT}}$ and $s \cdot \alpha_{\mathrm{AP}}$, respectively, resulting in a worst case model. We get (cf. (16)) and (19)):

$$\gamma_{\mathrm{MT,MT},s} = 10 \cdot \log_{10} \left(\frac{P_r^{\mathrm{lin}}}{P_i^{\mathrm{lin}} \cdot s \cdot \alpha_{\mathrm{MT}} + N_0^{\mathrm{lin}}} \right) \tag{30}$$

The angle φ of the dominated sector depends on s and is given by $\varphi = 2\,\pi/s$. In order to create the histograph of γ, we proceed similarly as in Lemma 3 with a different angular range

and the multiplication of the interference power in (30) by $s \cdot \alpha_{\mathrm{MT}}$:

$$f_{\gamma_{\mathrm{MT,MT},s}}(\gamma_1) = \sum_{(\rho_1,\phi_1,\rho_2,\phi_2)} \frac{\rho_1 \cdot \Delta\rho_1\, \Delta\phi_1 \;\cdot\; \rho_2 \cdot \Delta\rho_2\, \Delta\phi_2}{A_1 \cdot A_2} \tag{31}$$

$$\gamma_1 - \Delta\gamma < \gamma_{\mathrm{MT,MT},s}(\rho_1,\phi_1,\rho_2,\phi_2) \leq \gamma_1$$

where $\rho_1 \in [\rho_{\min}, R]$, $\rho_2 \in [\rho_{\min}, R]$, $\phi_2 \in [0, 2\pi[$ and $\phi_1 \in [-\pi/s, \pi/s]$.

The pdf $f_{\gamma_{\mathrm{AP,MT},s}}$ is determined similarly. Finally, we determine $f_{\gamma_{\mathrm{MT},s}}$ with $f_{\gamma_{\mathrm{MT,MT},s}}$ and $f_{\gamma_{\mathrm{AP,MT},s}}$ in the same manner as in (25) for $s = 1$.

Interference at the AP is treated slightly differently. Due to the fact that the AP in the observed cell is fixed, the SIR at the AP does not depend on the location. We use one more time the model for $s = 1$ for the whole observed cell and get the effective interference power by multiplying the interference power from a single interfering cell by $s \cdot \alpha_{\mathrm{AP}}$ for $f_{\gamma_{\mathrm{AP,AP},s}}$ and $s \cdot \alpha_{\mathrm{MT}}$ for $f_{\gamma_{\mathrm{MT,AP},s}}$, see (30).

The throughput $\mathcal{T}_{\mathrm{tot},s}$, finally, is determined in exactly the same way as defined in (27) through (29) by replacing $s = 1$ by the present s. Note that the model for $s = 1$ in section III-B is a special case of the model described in this section.

IV. Quantitative results

The results in this section will show that the maximum network throughput is not necessarily achieved at maximum transmit powers. For this purpose, outcomes from both, the theoretical and a simulation model will be presented. We will start with a brief introduction of the simulation model, show the plausibility of the results from the simulation model and then present the results.

A. Numerical simulator

The simulation model comprises a relatively detailed implementation of all the essential functions of the H2 standard. In contrast to the theoretical models, where no single packet is transmitted, the simulation model generates packets, performs all necessary actions in different protocol layers and transmits the packets via a common radio channel.

The simulation model and the theoretical model follow different paradigms, so we need to explain the differences between them. The theoretical model considers only the interference and the theoretically possible throughput of a Phy-mode after an ideal ARQ. However, the real H2 creates overhead in various layers. The most important sources of overhead are, [3]:

- The convergence layer (CL). The CL performs, among others, a segmentation and reassembly of packets which means that each packet gets some overhead in the form of a CL header. We have used the ethernet specific CL, [15].
- The DLC layer. Each MAC frame has some overhead, generated by the broadcast phase, the random access phase and the ARQ protocol overhead, [16].
- On the physical layer, some overhead is added by synchronisation headers, [5].

This means that only a percentage of the achievable throughput of the theoretical model can be used for actual user data transmission. A calculation of this percentage is presented in [17]. It depends on the number of active bidirectional connections a. We define for this purpose the overhead factor $ov(a)$ and the realistic throughput $\mathcal{T}_{\text{real}}$ of the theoretical model is computed by:

$$\mathcal{T}_{\text{real}} = \mathcal{T}_{\text{tot}} \cdot ov(a) \tag{32}$$

We have in all simulation runs four MTs moving in each radio cell, i.e. we have $a = 4$ active bidirectional connections with $ov(4) = 0.73$.

The theoretical model assumes that the MTs move equally distributed inside the radio cells. A movement model for circles with random waypoints on the border of the circle has been discussed in [18]. This model leads to a rather flat location probability over most of the circle area but increases at the circle border. We have developed a model without increase at the border which choses waypoints with probability p_R on the border and with probability $(1 - p_R)$ inside the circle. The waypoints inside the circle are exponentially distributed over ρ, starting at the border and decreasing towards the middle of the circle. The angle of waypoints is equally

distributed in the interval $[0, 2\,\pi[$. We have for the pdf of ρ:

$$f_\rho(\rho) = \begin{cases} p_R \cdot \delta(R) + (1-p_R)\frac{b}{R} \cdot e^{\frac{-b}{R}\cdot(R-\rho)}\,; & 0 < \rho \leq R \\ (1-p_R)\cdot e^{-b}\,; & \rho = 0 \\ 0\,; & \text{otherwise} \end{cases} \tag{33}$$

Investigations with with $b = 5$ and $p_R = 0.62$ show that this model achieves an almost perfectly equal location distribution in the observed circle areas.

B. Plausibility of simulation results

We show the plausibility by comparing the results generated by the simulator with those of the theoretical model. Both models assume high load conditions.

The general behaviour is, as expected, that in both models, the SIR in UL as well as in DL decreases for increasing s, regardless of the combination of $P_{t,\mathrm{AP}}$ and $P_{e,\mathrm{AP}}$. An example for the probability distribution of the SIR at the receiver for $R = 50\,\mathrm{m}$ and $D = 150\,\mathrm{m}$ with $P_{t,\mathrm{AP}} = 30\,\mathrm{dBm}$, $P_{e,\mathrm{AP}} = -43\,\mathrm{dBm}$ and $P_{t,\mathrm{MT},max} = 23\,\mathrm{dBm}$ for different s is shown in fig. 4 for UL and DL seperately[5]. In the UL, we have very good agreement between theory and simulation for all cases. The curves in the DL show very good agreement for the case of $s = 0$ and $s = 6$, whereas they differ slightly for $s = 1$. The curves for $s = 2$, $s = 3$ and $s = 4$, that are not shown in the graphs, match also excellently for this combination of $P_{t,\mathrm{AP}}$ and $P_{e,\mathrm{AP}}$. However, the match of theoretical and simulated cdf curves depends on $P_{t,\mathrm{AP}}$ and $P_{e,\mathrm{AP}}$, where the match is generally better for high values of $P_{t,\mathrm{AP}}$ and $P_{e,\mathrm{AP}}$. The difference between theory and simulation in fig. 4(b) for $s = 1$ is due to the fact that we use an idealised model for the scheduler in the theoretical model, whereas the scheduler in the simulator is non-ideal due to buffer state report delays owing to the MAC protocol, and the fact that the simulator scheduler additionally takes buffer states into account, which may vary over time and which are not considered in the theoretical model.

[5]For convenience of representation, we show the cumulative density function (cdf)

The throughput for the simulated and theoretical case versus s is shown in fig. 5 for $P_{t,\mathrm{AP}} = 30\,\mathrm{dBm}$ and $P_{e,\mathrm{AP}} = -43\,\mathrm{dBm}$. We have slightly higher throughput with the theoretical model for $s = 0$ which is due to the fact that the non-perfect ARQ implementation in the simulator operates at its limit. For all other s, we get almost identical throughput values. Again, this match depends on $P_{t,\mathrm{AP}}$ and $P_{e,\mathrm{AP}}$, where the match is better for high values of $P_{t,\mathrm{AP}}$ and $P_{e,\mathrm{AP}}$.

C. Selected results

All simulation results presented in this section were performed with a simulation duration of 600 s = 10 min, resulting in a standard deviation of 3.2% of throughput for different random generator start values. With the same motion patterns of MTs, the throughput has a standard deviation below 1%. All simulations, therefore, use the same motion pattern. The values for $P_{t,\mathrm{AP}}$ and $P_{e,\mathrm{AP}}$ are chosen from the ones defined by the H2 standard, [5].

The first question is whether a combination of $P_{t,\mathrm{AP}}$ and $P_{e,\mathrm{AP}}$ exists where the throughput reaches a maximum. High-load simulations and theoretical investigations have been performed with $R = 50\,\mathrm{m}$, $D = 150\,\mathrm{m}$ and $s = 4$ over $P_{t,\mathrm{AP}}$ and $P_{e,\mathrm{AP}}$ with $P_{t,\mathrm{MT},max} = 23\,\mathrm{dBm}$. Fig. 6 shows the graphs with the simulation and the theoretical model. The values chosen for $P_{t,\mathrm{AP}}$ and $P_{e,\mathrm{AP}}$ are a subset of the values permitted by the H2 standard, [5]. The throughput depends much more on $P_{t,\mathrm{AP}}$ than on $P_{e,\mathrm{AP}}$. Detailed investigation of the results show that both cases have a maximum at $P_{t,\mathrm{AP}} = P_{t,\mathrm{AP,opt}} = 24\,\mathrm{dBm}$, i.e. below the maximum values for $P_{t,\mathrm{AP}}$ and $P_{e,\mathrm{AP}}$[6]. The simulations have a much flatter graph than the theoretical investigations, which is due to the worst-case assumption for the DL in the theoretical model, see section III-C. Similar investigations have been performed with the same parameter set for $D = 245\,\mathrm{m}$ and $D = 335\,\mathrm{m}$.

The combinations of $P_{t,\mathrm{AP,opt}}$ and $P_{e,\mathrm{AP,opt}}$ with maximum throughput are listed in table III

[6]The differences between 24 and 27 dBm in the theoretical and between 21 and 24 in the simulation model are very small, so the data file has been consulted to enable precise statements. The contour lines on the bottom are helpful to see this result.

for both models together with $\mathcal{T}_{\max}$. The maximum is reached at the same $P_{t,\mathrm{AP,opt}}$ in both models for $D = 150\,\mathrm{m}$ and $D = 335\,\mathrm{m}$, but it is different for $D = 245\,\mathrm{m}$. The throughput, however, differs by less than 1% between $P_{t,\mathrm{AP,opt}} = 24\,\mathrm{dBm}$ and 27 dBm.

The values for $\mathcal{T}_{\max}$ differ slightly between the two models. This is because the simulation model takes some more effects into account which are not modelled by the theoretical model. Among them is the loss of broadcast information and the non-ideal ARQ implementation.

In order to investigate the influence of $P_{t,\mathrm{MT},max}$, theoretical calculations and simulations have been performed for the same scenario but with $P_{t,\mathrm{MT},max} = 30\,\mathrm{dBm}$. In this case, the network throughput reaches its maximum throughput at maximum transmit powers in both models. However, it can be assumed that most MTs will have $P_{t,\mathrm{MT},max} = 23\,\mathrm{dBm}$ rather than 30 dBm, so the results in table III seem to be more realistic.

V. Conclusions

The major achievement of this paper is the introduction of a novel theoretical model to evaluate the possible throughput perfomance of a wireless data network. This model has been applied to HIPERLAN type 2 systems. The results from the theoretical model have been compared with results from a simulation model and both models show good compliance. The results, obtained with a selected scheduling scheme, show that both models suggest that the maximum network throughput is not necessarily achieved when using maximum transmit powers but that it may be advisable to reduce them. Transmit powers can easily be adjusted by the owner of the network. Unfortunately, the optimum power setting depends on the distance D between APs which requires that the network owner has some notion of D. To find out the actual value of D, however, may not be easy due to the automatic frequency planning used in HIPERLAN type 2 and other modern systems.

The presented model is general in its approach but its application has been to HIPERLAN type 2 so far, considering a single scheduling scheme. It is desirable to develop similar models for other schedulers and for other wireless data network types. This involves mainly methods to

calculate the probability density function of the SIR at the receiver and a mathematical model of the influence of protocols, such as the MAC protocol.

REFERENCES

[1] D. Goodman and N. Mandayam, "Power Control for Wireless Data," *IEEE Personal Commun. Mag.*, April 2000.

[2] B. Walke, *Mobile Radio Networks*, 2nd ed. Wiley, 2002.

[3] J. Khun-Jush, G. Malmgren, P. Schramm, and J. Torsner, "HIPERLAN type 2 for Broadband Wireless Communication," *Ericsson review*, 2000. [Online]. Available: http://www.ericsson.com/review

[4] M. Radimirsch and V. Vollmer, "HIPERLAN Type 2 Standardisation - an Overview," in *Proc. European Wireless Conference*, Munich, Germany, 1999.

[5] *BRAN; HIPERLAN Type 2; Physical (PHY) Layer Specification*, ETSI Technical Specification 101 475, 2nd edition, 2001. [Online]. Available: http://www.etsi.org

[6] S. Feldmann and M. Radimirsch, "A novel approximation method for error rate curves in radio communication systems," in *Proc. of PIMRC*, Lisbon, Portugal, Sept. 2002.

[7] B. Chen, R. Grünheid, and H. Rohling, "Scheduling Policies for Joint Optimisation of DLC and Physical Layer in Mobile Communication Ssytems," in *Proc. of PIMRC*, Lisbon, Portugal, Sept. 2002.

[8] Z. Lin, G. Malmgren, and J. Torsner, "System performance analysis of link adaptation in HiperLAN type 2," in *Proc. of 52nd VTC (Fall)*, vol. 4, Boston, MA , USA, 2000.

[9] A. Krämling, M. Siebert, M. Lott, and M. Weekerle, "Interaction of Power Control and Link Adaptation for Capacity Enhancement and QoS Assistance," in *Proc. 13th PIMRC*, vol. 2, Lisbon, Portugal, Sept. 2002.

[10] M. Radimirsch, "An algorithm to combine link adaptation and transmit power control in HIPERLAN type 2," in *Proc. of PIMRC*, Lisbon, Portugal, Sept. 2002.

[11] G. Halls, "HIPERLAN: the high performance radio local area network standard," *IEE Electronics & Communication Engineering Journal*, vol. 6, no. 6, Dec. 1994.

[12] J. Proakis, *Digital Communications*, 3rd ed. McGraw-Hill International Editions, 1995.

[13] M. Radimirsch, "Optimisation of Throughput and Energy Efficiency in HIPERLAN Type 2 Networks," Ph.D. dissertation, Institut für Allgemeine Nachrichtentechnik, Universität Hannover, May 2004, (to be published at Shaker Verlag, Aachen, Germany).

[14] A. Papoulis, *Probability, Random Variables, and Stochastic Processes*, 3rd ed. McGraw-Hill International Editions, 1991.

[15] *BRAN; HIPERLAN Type 2; Packet based Convergence Layer; Part 2: Ethernet Specific Convergence Sublayer*, ETSI Technical Specification 101 493-1, 2001. [Online]. Available: http://www.etsi.org

[16] *BRAN; HIPERLAN Type 2; Data Link Control (DLC) Layer; Part 1: Basic Data Transport Function*, ETSI Technical Specification 101 761-1, 2nd edition, 2001. [Online]. Available: http://www.etsi.org

[17] B. Walke *et al.*, "IP over Wireless Mobile ATM - Guaranteed Wireless QoS by HiperLAN/2," *Proc. IEEE*, vol. 89, no. 1, Jan. 2001.

[18] C. Bettstetter and C. Wagner, "The Spatial Node Distribution of the Random Waypoint Mobility Model," in *Proceedings GI Workshop Mobile Ad-Hoc Netzwerke*, Ulm, Germany, Mar. 2002.

APPENDIX I
PROOF OF LEMMA 1

The SIR is given by $P_{r,\mathrm{AP}} - N_0$, where $P_{r,\mathrm{AP}}$ is defined in (10). The function $f^{(1)}_{\gamma_{\mathrm{AP},0}}(\gamma)$ in (11) describes the constant part of $P_{r,\mathrm{AP}}$ in (10). The terminals are equally distributed in the circle with radius R around the AP, with minimum distance $\rho_{\min}$. Due to the symmetry of the circle, the SIR is merely a function of the distance ρ to the AP. The pdf $f_\rho(\rho)$ of the location inside

the circle increases proportionally with ρ:

$$f_\rho(\rho) = \frac{2}{R^2 - \rho_{\min}^2} \cdot \rho \tag{34}$$

The pdf of γ of the constant part is given by:

$$f^{(1)}_{\gamma_{\mathrm{AP},0}}(\gamma) = \delta(P_{e,\mathrm{AP}} - N_0) \cdot \int_{\rho_{\min}}^{\min\{R,\, 10^{\left(P_{t,\mathrm{MT},max} - a_2 - P_{e,\mathrm{AP}}\right)/b_2}\ \mathrm{m}\}} f_\rho(\rho)\, d\rho \tag{35}$$

The upper limit of the integral is either determined by the end of the constant part in (10) or by the radius R. Evaluation of the integral yields $f^{(1)}_{\gamma_{\mathrm{AP},0}}$ according to (11).

The lower part of (10), representing the decreasing part of the graph in (10), is the basis for $f^{(2)}_{\gamma_{\mathrm{AP},0}}(\gamma)$ in (12). If a random variable x has the pdf $f(x)$ and $y = g(x)$ is a function of x, then the pdf of y is given by [14, p.93]:

$$f_y(y) = \frac{f_x(x)}{|g'(x)|}. \tag{36}$$

In our case, y is given by γ, x by ρ with its pdf in (34) and $y = g(x)$ by $\gamma_{\mathrm{AP},0} = P_{r,\mathrm{AP}} - N_0$ with $P_{r,\mathrm{AP}}$ in the lower part of (10). We start with $P_{r,\mathrm{AP}}$ and solve $\gamma_{\mathrm{AP},0} = P_{r,\mathrm{AP}} - N_0$ for ρ. Inserting everything in (36) results in $f^{(2)}_{\gamma_{\mathrm{AP},0}}(\gamma)$ in (12).

$\triangle$

APPENDIX II

FIGURES

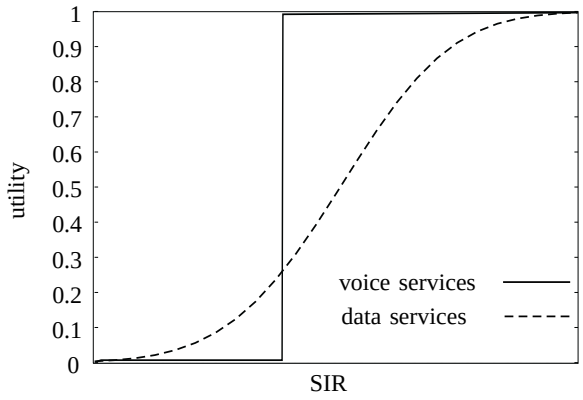

Fig. 1. Utility function for voice services and for data services

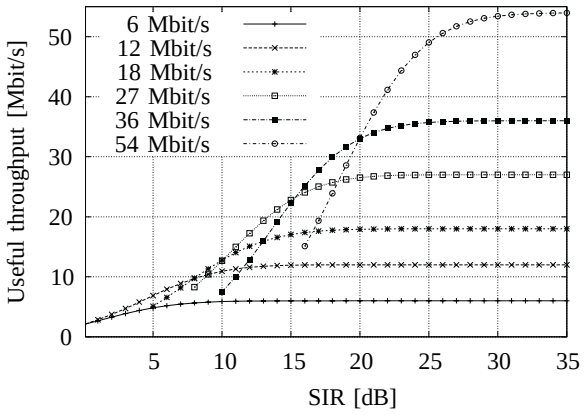

Fig. 2. Theoretically achievable useful throughput with the Phy-mode PM as Parameter

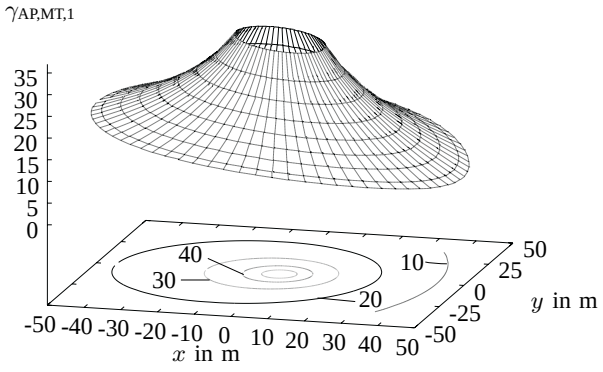

Fig. 3. $\gamma_{\text{AP, MT}}$ for $s = 1$ with countour lines on the base; ($R = 50\,\text{m}$, $D = 125\,\text{m}$)

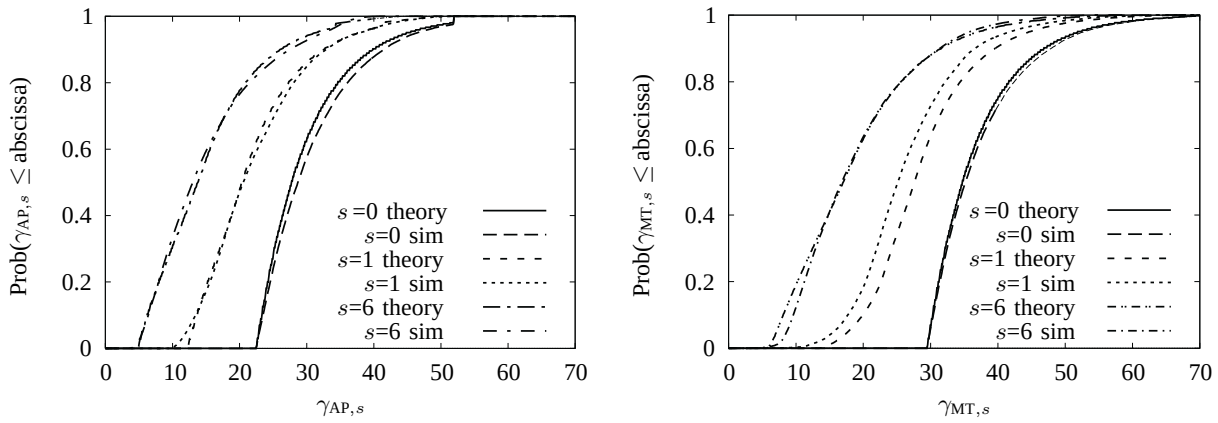

(a) (b)

Fig. 4. cdf of γ (a) at the AP, (b) at MTs für $a = 4$ MTs from simulation and theoretical model with s as Parameter ($R = 50\,\mathrm{m}$, $D = 125\,\mathrm{m}$)

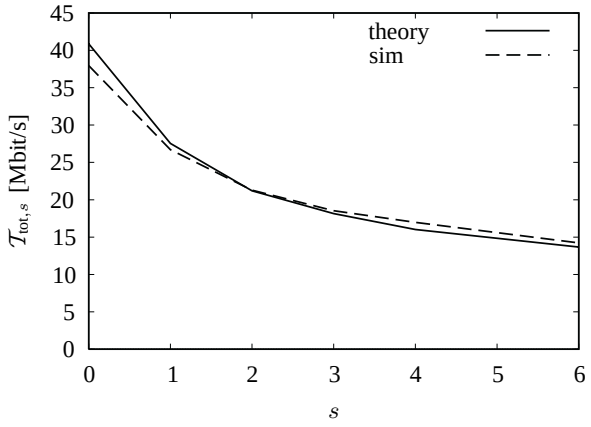

Fig. 5. $\mathcal{T}_{\mathrm{tot},s}$ versus s for $a = 4$ MTs from simulation and theoretical model ($R = 50\,\mathrm{m}$, $D = 150\,\mathrm{m}$)

APPENDIX III

TABLES

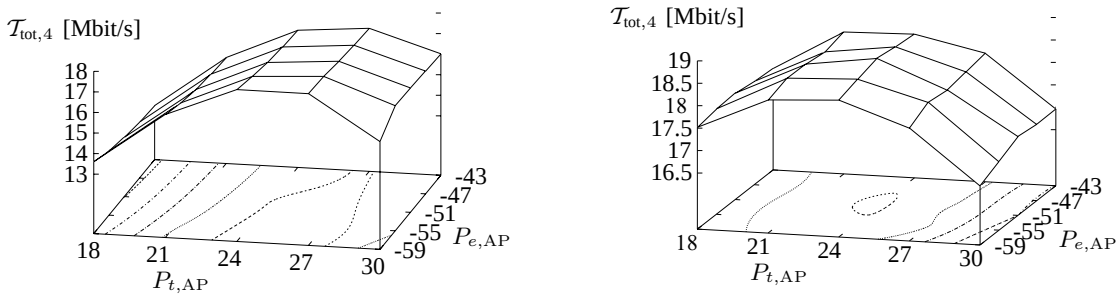

(a) (b)

Fig. 6. $\mathcal{T}_{\text{tot},4}$ versus $P_{t,\text{AP}}$ and $P_{e,\text{AP}}$ for $a = 4$ MTs from (a) theoretical and (b) simulation model ($R = 50\,\text{m}$, $D = 150\,\text{m}$, $s = 4$)

TABLE I

TOTAL THROUGHPUT VALUES $\mathcal{T}_{\text{TOT, UL}}$ FOR VARIOUS $P_{e,\text{AP}}$ AND R WITH A SINGLE CELL (ALL VALUES IN MBIT/S)

	R/m			
$P_{e,\text{AP}}/\text{dBm}$	30	50	75	100
-43	53,9	50,8	39,0	30,0
-51	53,9	50,8	39,0	30,0
-63	53,8	50,8	39,0	30,0
-67	52,5	50,3	38,8	29,9
-71	47,0	46,6	37,3	29,2

TABLE II

TOTAL THROUGHPUT VALUES $\mathcal{T}_{\text{TOT, DL}}$ FOR VARIOUS $P_{t,\text{AP}}$ AND R WITH A SINGLE CELL (ALL VALUES IN MBIT/S)

	R/m			
$P_{t,\text{AP}}/\text{dBm}$	30	50	75	100
30	54,0	53,9	51,8	44,1
21	53,7	47,2	35,0	25,9
12	44,4	29,5	16,9	10,1
3	26,4	12,5	5,2	2,8
-6	10,4	3,4	1,4	0,8

TABLE III

COMBINATION OF $P_{t,\text{AP}}$ AND $P_{e,\text{AP}}$ AT WHICH $\mathcal{T}_{\max}$ IS ACHIEVED FOR THEORETICAL AND SIMULATION MODEL

	Theory			Simulation		
D [m]	$P_{t,\text{AP}}$ [dBm]	$P_{e,\text{AP}}$ [dBm]	$\mathcal{T}_{\max}$ [Mbit/s]	$P_{t,\text{AP}}$ [dBm]	$P_{e,\text{AP}}$ [dBm]	$\mathcal{T}_{\max}$ [Mbit/s]
150	24	-55	17.74	24	-51	18.57
245	27	-59	30.14	24	-55	28.96
335	27	-63	36.28	27	-55	33.72